

# Lawrence Berkeley National Laboratory

## Lawrence Berkeley National Laboratory

### Title

Dynamics of H abstraction from alcohols (CH<sub>3</sub>OH, C<sub>2</sub>H<sub>5</sub>OH and 2-C<sub>3</sub>H<sub>7</sub>OH) using velocity map imaging in crossed molecular beams

### Permalink

<https://escholarship.org/uc/item/8dx1n4rq>

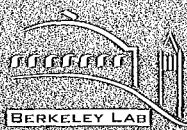
### Author

Ahmed, M.

### Publication Date

1999-09-01

Peer reviewed



ERNEST ORLANDO LAWRENCE  
BERKELEY NATIONAL LABORATORY

**Dynamics of H Abstraction from  
Alcohols ( $\text{CH}_3\text{OH}$ ,  $\text{C}_2\text{H}_5\text{OH}$  and  
2- $\text{C}_3\text{H}_7\text{OH}$ ) Using Velocity Map  
Imaging in Crossed Molecular Beams**

Musahid Ahmed, Darcy S. Peterka, and Arthur G. Suits

**Chemical Sciences Division**

September 1999

Submitted to  
*Physical Chemistry*  
*Chemical Physics PCCP*

REFERENCE COPY |  
Does Not |  
Circulate |  
Bldg. 50 Library - Ref.  
Lawrence Berkeley National Laboratory

#### **DISCLAIMER**

This document was prepared as an account of work sponsored by the United States Government. While this document is believed to contain correct information, neither the United States Government nor any agency thereof, nor The Regents of the University of California, nor any of their employees, makes any warranty, express or implied, or assumes any legal responsibility for the accuracy, completeness, or usefulness of any information, apparatus, product, or process disclosed, or represents that its use would not infringe privately owned rights. Reference herein to any specific commercial product, process, or service by its trade name, trademark, manufacturer, or otherwise, does not necessarily constitute or imply its endorsement, recommendation, or favoring by the United States Government or any agency thereof, or The Regents of the University of California. The views and opinions of authors expressed herein do not necessarily state or reflect those of the United States Government or any agency thereof, or The Regents of the University of California.

Ernest Orlando Lawrence Berkeley National Laboratory  
is an equal opportunity employer.

**Dynamics of H Abstraction from Alcohols  
(CH<sub>3</sub>OH, C<sub>2</sub>H<sub>5</sub>OH and 2-C<sub>3</sub>H<sub>7</sub>OH) Using Velocity  
Map Imaging in Crossed Molecular Beams**

Musahid Ahmed, Darcy S. Peterka, and Arthur G. Suits

Chemical Sciences Division  
Ernest Orlando Lawrence Berkeley National Laboratory  
University of California  
Berkeley, California 94720

September 1999



Correspondence and proofs:  
Dr. Arthur Suits agsuits@lbl.gov  
MS 6-2100 Berkeley Lab  
1 Cyclotron Rd  
Berkeley CA 94720 USA

**Dynamics of H abstraction from alcohols (CH<sub>3</sub>OH, C<sub>2</sub>H<sub>5</sub>OH and  
2-C<sub>3</sub>H<sub>7</sub>OH) using velocity map imaging in crossed molecular beams.**

Musahid Ahmed, Darcy S. Peterka and Arthur G. Suits

*Chemical Sciences Division  
Ernest Orlando Lawrence Berkeley National Laboratory  
Berkeley, CA 94720*

---

**ABSTRACT**

The crossed beam reactions of ground state Cl (<sup>2</sup>P<sub>3/2</sub>) atoms with alcohols (CH<sub>3</sub>OH, C<sub>2</sub>H<sub>5</sub>OH and 2-C<sub>3</sub>H<sub>7</sub>OH) have been studied using the technique of velocity map imaging (VELMI). The corresponding hydroxyalkyl radical was detected via single photon ionization using 157 nm laser light. The double differential cross sections were obtained at collision energies of 8.7 kcal/mol for methanol, 6.0 and 9.7 kcal/mol for ethanol, and 11.9 kcal/mol for 2-propanol. In all cases, the scattering was predominantly in the backward-sideways direction suggesting direct rebound dynamics, with varying amounts of sideways-scattering. In the case of methanol, the angular distributions were predominantly in the sideways-backward direction with respect to the incoming alcohol beam. Scattering was into the backward hemisphere at the lower collision energy for ethanol, with enhancement of sideways scattering with an increase in collision energy. Isopropanol gave scattering predominantly in the backward direction. Coupling between the translational energy and angular distributions was particularly significant for ethanol at the lower collision energy. All of the translational energy distributions peaked at about 6 kcal/mol and on average 30-40% of the available energy was deposited into product translation for all the alcohols studied. These results are contrasted with previous H abstraction studies performed on Cl-hydrocarbon systems. A case is made for the technique of vacuum ultraviolet one-photon ionization in conjunction with VELMI being useful in studying the reaction dynamics for many polyatomic systems.

---

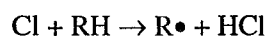
## INTRODUCTION

Abstraction reactions of hydrogen atoms from hydrocarbons are of great importance in combustion and atmospheric chemistry. This is reflected in numerous publications where the kinetics of these processes have been probed in detail. While rate information provides some insight into the mechanisms of these reactions, it is the dynamics that provides a deeper understanding. For example, free radical abstraction of hydrogen atoms from saturated hydrocarbons and the differing propensities for reaction of primary, secondary, or tertiary H atoms, as well as differing dynamics underlying these pathways, are important for a detailed understanding of combustion chemistry. With the advent of laser technology and development of new techniques in studying such processes, there has been an explosion of studies, particularly for the reactions of O and Cl with saturated hydrocarbons.

The earliest study of the dynamics of H abstraction from saturated hydrocarbons can be traced back to two seminal papers by Andresen and Luntz<sup>1,2</sup>, wherein they probed the dynamics of O(<sup>3</sup>P) with a variety of saturated hydrocarbons (neopentane, cyclohexane, and isobutane) using laser induced fluorescence (LIF) in conjunction with crossed molecular beams. They found that the resultant OH rotational state distributions were nearly identical for all the hydrocarbons and decrease rapidly from a peak at the lowest rotational level, suggesting strong dynamical constraints favoring collinearity in the critical region along the reaction pathway. The trends that they observed for the OH rotational distribution have been confirmed in all subsequent studies of H abstraction dynamics – that the newly formed hydride products, regardless of the identity of the hydrocarbon or the attacking atom, are formed rotationally cold. Furthermore they found that the vibrational state distribution of OH depends markedly on the type of hydrogen abstracted, with vibrational excitation increasing dramatically across the series primary to secondary to tertiary, correlating with the increasing exothermicity of the reaction. They interpreted this dynamic behavior as a shift from a repulsive towards a more attractive surface across the series of hydrocarbons studied.

Subsequently the reactions of O(<sup>3</sup>P) with a number of organic compounds were studied using similar techniques by a number of groups – notably Kleinermands and Luntz<sup>3-5</sup> and Whitehead and co-workers<sup>6,7</sup>. Very recently McKendrick and co-workers<sup>8,9</sup> have reinvestigated the reactions of oxygen with a series of hydrocarbons. They confirmed the previous results of Andresen and Luntz, and went on to investigate the reaction of O(<sup>3</sup>P) with CH<sub>4</sub> and C<sub>2</sub>H<sub>6</sub>. They found similar low levels of rotational energy release, suggesting that the previously proposed strong collinear constraint also applied to the smaller hydrocarbons.

The abstraction reaction



leads to the formation of a chain-propagating organic hydrocarbon radical whose properties and chemistry are of importance in combustion, atmospheric, and interstellar processes. Zare and co-workers<sup>10-12</sup> have pioneered the study of the dynamics of Cl atom reactions with a variety of hydrocarbons using the “photoloc” technique, providing state-resolved differential cross sections for these reactions. The HCl rotational distribution from the reaction of Cl with vibrationally excited methane showed the characteristic cold rotational distribution but the scattering was predominantly forward, especially for the vibrationally excited product. Since these experiments were performed on the state-to-state level, the authors showed that even though all the rotational distributions were relatively cold, for the highly excited HCl product, the higher J values were associated with greater back-scattering. Furthermore, with the photoloc technique stereodynamic information can be extracted from the experimental results. The authors reported a significant steric effect; reactions yielding HCl (v=1) were favored by perpendicular approach of the Cl atoms to the excited C-H stretch. This observation was explained by invoking a hard-sphere model (line-of-centers) in which reaction is only possible for small impact parameter collisions. They also argued that the association of low rotational excitation with a collinear transition state, as adduced by Andresen and Luntz in the O(<sup>3</sup>P) reactions and Flynn and co-workers<sup>13</sup> for the Cl-



$C_6D_6$  reaction, is strictly appropriate only when there is impulsive energy release in the reaction. For the Cl-methane( $v=1$ ) case, the forward scattered HCl, which is the dominant product, the cold rotational distribution were attributed simply to stripping like mechanism involving large impact parameter collisions.

For the Cl- $CD_4$  and Cl- $C_2D_6$  systems<sup>14</sup>, both showed scattering behavior described by the previously mentioned line-of-centers model and both yielded rotationally cold DCI product with little energy in the alkyl fragment. However the product polarizations differed greatly for the two reactions. For the Cl+ $CD_4$  reaction,  $J_{DCL}$  was maximally aligned perpendicular to the axis close to the product scattering direction, while for the Cl+ $C_2D_6$  case the  $J_{DCL}$  was half-maximally aligned perpendicular to the line-of-centers direction. The authors interpreted these results in terms of the location of the D-atom transfer along the reaction coordinate, positing that the D-atom transfer for the methane reaction occurs late in the reactive process, while for ethane the reaction occurs earlier near the distance of closest approach. The authors argue that this dynamical behavior is the cause of the large differences in the Arrhenius pre-exponential factors for the two reactions. Previously Zare's group used 2+1 REMPI to study the HCl distributions and differential cross-sections arising from the reaction of Cl with different hydrocarbons. Very recently, Kandel et al<sup>15</sup> probed the differential cross-section for the Cl+ $C_2H_6 \rightarrow Cl+C_2H_5$  reaction, using a 2+1 REMPI scheme to detect the heavier hydrocarbon radical product. These results were identical to the ones measured using the HCl detection scheme<sup>16</sup>.

While Zare and co-workers have concentrated their efforts on the reaction of Cl with small hydrocarbons, Varley and Dagdigian<sup>17-19</sup> carried out a detailed investigation of the reactions with propane, isobutane, selectively deuterated propane and also methane. State-resolved differential cross-sections were obtained using a technique similar to Zare's photoloc approach – HCl was predominantly backscattered in the isobutane reaction, and the vibrational population ratios were very similar for propane and isobutane. Andresen and Luntz observed very

different behaviour for the O(<sup>3</sup>P) reaction. Varley and Dagdigian's result for partially deuterated propane showed abstraction of the D atoms (as the primary substituents) led to sideways scattered DCI product, while abstraction of the H atom (secondary substituents) led to a more isotropic angular distribution, yet still favoring the backward direction.

Elegant as these state-resolved experiments are, one must exercise caution in interpreting the results involving polyatomic systems. In the experiments of Varley and Dagdigian as well as the photoloc experiments, the distributions obtained are largely blind to the internal energy in the undetected product. Often the assumption is made that the undetected product is internally cold, an assumption that may not be valid. Suits and co-workers have employed a novel alternative technique to probe the hydrocarbon radicals formed in the abstraction reactions of Cl with hydrocarbons. They used the crossed molecular beam technique in conjunction with tunable VUV synchrotron radiation for product photoionization to study the dynamics of Cl reactions with propane<sup>20</sup> and pentane<sup>21</sup>. The use of tunable undulator radiation offered them a unique combination of universality and selectivity in product detection which was not possible with traditional electron impact ionization normally used in such crossed beam studies. The results for propane showed two distinct reaction mechanisms that depended on the impact parameter of the reactive collision. Large impact parameter collisions proceed via a stripping mechanism resulting in forward-scattered products with very little momentum change in going from reactant to product. The authors argue that the stripping reactions are most likely dominated by abstraction of secondary hydrogen atoms. The second mechanism, involving smaller impact parameter collisions, leads to direct reaction consistent with a preference for a collinear transition state geometry, C-H-Cl.

In the case of pentane, Hemmi and Suits<sup>21</sup> found that the energy and angular distributions were strongly coupled, with the forward scattered pentyl radical formed extremely cold, while the backscattered radicals were formed leaving nearly 15 kcal/mol in internal energy

of the products. The results for the forward scattered products was largely consistent with previous studies of Cl-hydrocarbon reaction dynamics (spectator-stripping mechanism). In contrast the results for the backscattered products showed a much smaller fraction of the available energy in translation, compared with earlier studies. They invoked the direct involvement of the carbon skeleton in the collision process. Pentane contains a higher density of states compared to propane; furthermore there is an excellent match between the collision time and the bending vibrational period, allowing efficient coupling between the collision energy and the internal modes of the molecule.

While there have been a number of detailed dynamical studies performed on H abstractions from saturated hydrocarbons, it is surprising that analogous studies of H abstraction from alcohols are so rare. Alcohol oxidation has broad practical significance. Alcohols, saturated and unsaturated, are emitted into the atmosphere by vegetation<sup>22</sup>. These biogenic emissions play an important role in the chemistry of the troposphere, especially in rainforest eco-systems such as the Amazon. Saturated alcohols have long been used in large quantities as industrial solvents. Most importantly, from the earliest days of the internal combustion engine - N. A. Otto used ethanol in his classical combustion engine tests in 1897 - alcohols have been used as fuels and fuel additives. Recently there has been greatly renewed interest in alcohol based combustion systems<sup>23</sup> as an alternative to gasoline since the former are thought to be environmentally more benign<sup>24</sup>.

There have been a few cases in the literature where the dynamics of reaction of electronically excited atoms with alcohols have been documented. Goldstein and Wiesenfeld<sup>25</sup> studied the reaction of O(<sup>1</sup>D) with methanol and ethanol and its deuterated analogues and characterised the OH and OD product ratios and vibrational distributions using LIF. Their results show that the primary site of O(<sup>1</sup>D) attack upon the alcohols is the O-H bond, although some attack upon the C-H bond was also observed. They suggested an insertion/elimination mechanism

and concluded that abstraction processes were minor based on the low vibrational excitation of OH(OD). Very recently Umemoto *et al*<sup>26</sup> examined the reaction pathways of N(<sup>2</sup>D) with methanol and its isotopomers using LIF pump-and-probe techniques. They observed ground state NH and OH radicals with the nascent state distributions of these radicals being non-statistical, suggesting that the intermediate decomposes before energy randomization. These examples have been included here to contrast the differences in the dynamics of electronically excited atoms and ground state reactants. The only dynamic study to-date of ground state reactions with alcohols was performed by Neumark and co-workers<sup>27</sup>. They studied fluorine atom reactions with methanol and ethanol using negative ion transition state spectroscopy. It should be pointed out that the dynamics of F atom reactions with alcohols are not representative across the halogen series, since the large exothermicity associated with these opens channels are not available to other halogens or hydroxyl radicals.

We have undertaken a series of experiments to study the dynamics of H abstraction from alcohols using crossed molecular beams in conjunction with velocity map imaging; a preliminary report of our study of the methanol reaction has recently been submitted<sup>28</sup>. Ion imaging is a multiplexing method which provides simultaneous detection of all recoil velocities, both speed and angle, for the detected product<sup>29</sup>. Furthermore, the images can be directly deconvoluted to yield the velocity-flux contour maps which summarize the dynamics. This deconvolution does not require the simplifying assumption of uncoupled translational energy and angular distributions usually employed in analyzing reactive scattering experiments, so the imaging experiments thus directly reveal the genuine double differential cross sections ( $d^2\sigma/dE_T d(\cos\theta)$ ). Another advantage of the imaging technique, particularly in the present studies, is the absence of any kinematic limitations on the reactions. Products scattering much faster or much slower than the beams themselves may be easily detected.

Very recently we performed the first experiment utilizing velocity map imaging<sup>30</sup> (VELMI) to study the reaction dynamics of the  $O(^1D) + D_2 \rightarrow OD + D$  system<sup>31</sup>. Despite the advantages of the crossed-beam imaging technique, there have been relatively few such studies<sup>32,33</sup>. Almost all have been performed using 1+1 REMPI. While there are many more species that could be detected using 2+1 REMPI, sensitivity issues (small interaction volume owing to the tight laser focus, low cross-sections) have precluded their use except in a few recent cases of inelastic scattering. Recently, groups at Cornell<sup>34-37</sup> and Berkeley<sup>20,21</sup> have used VUV radiation to perform one-photon photoionization detection of polyatomic radical fragments from bimolecular reactions. The Berkeley group as mentioned earlier used tunable synchrotron radiation with a “traditional” crossed beam configuration to detect hydrocarbon radicals formed in bimolecular reactions of Cl with propane and n-pentane. The Cornell group has pioneered the use of 157nm radiation generated by the F<sub>2</sub> excimer laser to photoionize products formed in metal-hydrocarbon bimolecular reactions. We adapted the latter technique to our crossed-beam velocity map imaging experiment. Here we present results for the reaction of Cl with methanol, ethanol, and 2-propanol.

## EXPERIMENTAL

The crossed molecular beams apparatus (Fig. 1) has been described in detail in recent publications from our group<sup>38,31</sup>. The Cl beam was generated by photodissociation of oxalyl chloride [(ClCO)<sub>2</sub>] seeded in He, using the 193 nm output of a ArF excimer laser (60 mJ, 10 Hz Lambda Physik) at the nozzle of a Proch-Trickl piezoelectric pulsed valve<sup>39</sup>. The molecular beam of (ClCO)<sub>2</sub> was generated by passing helium through a bubbler containing oxalyl chloride, held at 6° C. The photodissociation dynamics of oxalyl chloride have recently been examined in our laboratory and photodissociation at 193nm yields predominantly Cl, Cl\* and CO.<sup>40</sup> The Cl atom beam velocity and spread was monitored using (2+1) REMPI of Cl(<sup>2</sup>P<sub>3/2</sub>) via the 4p<sup>2</sup>D<sub>3/2</sub>

$\leftarrow\leftarrow 3p^2P_{3/2}$  transition at 235.336nm.<sup>41</sup> The UV photodissociation of oxalyl chloride also generates the spin-orbit excited  $\text{Cl}^*(^2P_{1/2})$  which was monitored using the  $4p^2P_{1/2} \leftarrow\leftarrow 3p^2P_{1/2}$  transition at 235.205nm. The  $\text{Cl}^*/\text{Cl}$  ratio was 1:50 and 1:62 for oxalyl chloride seeding in He and Ar respectively, or better than 98% ground state Cl, using relative linestrengths for the transitions as discussed in reference 26. We believe the efficient quenching is likely induced by many Cl-CO collisions. The alcohol (methanol, ethanol, 2-propanol) seeded 2% in He was expanded through another Proch-Trickl pulsed valve, collimated by a single skimmer and the beams were allowed to interact on the axis of the velocity focusing time-of-flight mass spectrometer. For the ethanol experiments the collision energy was reduced by seeding the oxalyl chloride in Ar.

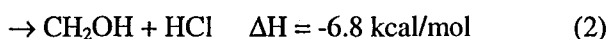
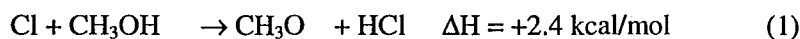
Light from a 157nm excimer laser (1-2 mJ, 10Hz, Lambda-Physik) was focussed loosely into the interaction region of the two crossed beams and used to ionize the hydroxyalkyl radical reaction product. The ions were accelerated toward a 80-mm diameter dual microchannel plate (MCP) detector coupled to a fast phosphor screen (P-47) and imaged on a fast scan charge-coupled device camera with integrating video recorder (Data Design AC-101M). Camera threshold and gain were adjusted in conjunction with a binary video look-up table to perform integration of single ion hits on the MCP free of video noise. The recorded image is actually a 2-dimensional (2-D) projection of the nascent 3-dimensional (3-D) velocity distribution, and established tomographic techniques<sup>29</sup> were used to reconstruct the 3-D distribution. Typical accumulation time for a single collision energy was about 30 minutes.

## RESULTS

Fig. 2 shows a raw image of the product formed at mass 45,  $\text{CH}_3\text{CHOH}$ , from the reaction of Cl with ethanol probed with 157nm laser light. The relative velocity vector is vertical in the plane of the figure, and the Newton diagram for the scattering process has been superimposed on the image. There is substantial photodissociation of ethanol at 157nm which also produces  $\text{CH}_3\text{CHOH}$ . This shows up as the small ring centered at the ethanol beam. As is

immediately apparent from the image, this creates a problem in extracting information for forward scattering relative to the incoming alcohol beam. We subtracted an image recorded with the 193nm laser off from a reactive scattering image to remove the photodissociation contribution from the reactive scattering image. Unfortunately, the intense photochemical signal creates substantial noise and corresponding uncertainty in the reactive flux formed between 0-50° (as indicated in the subsequent data images.) However we can extract the full double-differential cross-section reliably from the rest of the image.

The reaction of Cl with methanol can proceed via two channels:



channel (1) and (2) forming the methoxy and hydroxymethyl radicals respectively. The branching ratio for the latter channel has been found experimentally to be close to unity, 0.95<sup>42</sup>. The ionization potential for CH<sub>3</sub>O is 10.42 eV<sup>43</sup> (and the CH<sub>3</sub>O<sup>+</sup> ion is unstable<sup>44</sup>) so that we will not be sensitive to this channel. However the I.P. for CH<sub>2</sub>OH is 7.56 eV<sup>45</sup>, so that single photon ionization using the 157nm laser light (7.9 eV) will readily probe this product from channel (2) above. Fig. 3 shows an image of the product formed at mass 31, CH<sub>2</sub>OH<sup>+</sup>, from the reaction of Cl with methanol. The relative velocity vector is vertical in the plane of the figure, and the Newton diagram for the scattering process has been superimposed on the image.

At a collision energy  $E_{\text{coll}}$  of 8.7 kcal/mol, there is 15.5 kcal/mol energy available to be distributed into translation and the internal energy of the products. The outer ring in Fig. 3 shows the maximum recoil speed allowed for the CH<sub>2</sub>OH radical; there is reactive flux virtually to the limit of available energy in the sideways and backward direction. The cylindrical symmetry of the experiment justifies the use of the inverse Abel transform method to reconstruct the full 3D distributions, so that this analysis is, in effect, a direct inversion of the experimental data. The c.m. angular distributions  $[d\sigma/d(\theta)]$ , extracted from the images are shown in the lower panel of

Fig. 4. There is substantial sideways scattering – the ratio of sideways (45°-135°) to backward (135°-180°) is 1.75. The upper panel in Fig. 4 shows the translation energy distribution obtained from the reconstructed data at  $E_{\text{coll}} = 8.7$  kcal/mol. The maximum available energy is indicated in the figure. The average translational energy released is 6.1 kcal/mol which is 39% of the available energy.

The abstraction of a H atom from ethanol by the Cl atom can give rise to three different radicals as shown below:



In our experiment we will not observe the ethoxy radical channel (5), since its ionization energy of  $10.29 \text{ eV}^{46}$  is way above that available from a 157nm photon (7.89 eV). The ionization energies for the 1-hydroxyethyl and 2-hydroxyethyl radical formed in process (3) and (4) are  $6.64 \text{ eV}^{47}$  and  $\sim 8.2 \text{ eV}^{46}$  respectively. However the I.E. for 2-hydroxyethyl is by no means conclusive. Ruscic and Berkowitz<sup>46</sup> quote a figure of  $8.18 \pm 0.08$ , but they infer an I.P. of  $\sim 7.7 \text{ eV}$  depending on the thermodynamic cycle and bond dissociation energies employed in generating the result. A G-2 theoretical result<sup>48</sup> posits 7.58 eV as the adiabatic ionization energy for the 2-hydroxyethyl radical. Khatoon *et al.*<sup>49</sup> carried out an end product analysis experiment to measure the rates of this reaction and also derive the branching ratio for the formation of the three different radicals. They conclude for the reaction of Cl with alcohols no abstraction from the OH group was observed and that the abstraction from the alkyl groups followed the thermodynamically favoured route by forming mainly secondary radicals. With this in mind we can tentatively say that the mass 45 detected is the 1-hydroxyethyl radical.

Reactive scattering experiments with ethanol were performed at two collision energies  $E_{\text{coll}} = 6.0$  kcal/mol and 9.7 kcal/mol. Fig. 5A shows the raw image for 6.0 kcal/mol and as



indicated previously for the methanol results the Newton diagram is superimposed on the image. The reactive flux is predominantly in the backward hemisphere. When the collision energy is increased to 9.7 kcal/mol, there is enhanced sideways scattering, and the raw image shown in Fig. 5B begins to resemble the methanol system. However for ethanol at both collision energies the reactive flux does not extend out to the thermodynamic limit. The average translational energy release is 38 and 32% of the available energy for  $E_{\text{coll}} = 6.0$  kcal/mol and 9.7 kcal/mol, respectively. The upper panel in Fig. 6 shows the translational energy distribution obtained from the reconstructed data at  $E_{\text{coll}} = 6.0$  kcal/mol and 9.7 kcal/mol, respectively. The corresponding angular distributions are shown in the lower panel. As was apparent in the raw images, we see a large enhancement in sideways scattering with an increase in collision energy. There is also substantial coupling between translational energy release and corresponding angular distributions. Fig 7 compares the translational energy release for the sideways (50-130°) to backward (130-180°) components at a collision energy of 6.0 kcal/mol. The average energy release for the sideways scattering is 4.7 kcal/mol; the backward scattering is faster with 6.6 kcal/mol released as translational energy.

A image recorded at mass 59, corresponding to  $(\text{CH}_3)_2\text{COH}^+$  is shown in fig. 8. The ionization energies for the possible product radicals are not available, except for 9.2 eV for the product of hydroxyl H abstraction, the 1-Methyl ethoxy radical<sup>50</sup>. However, analogy to the systems above suggest a much lower I.E. for the  $(\text{CH}_3)_2\text{COH}$  radical, and we believe this to be the most likely candidate for our detected product in this reaction. The scattering is predominantly in the backward hemisphere and the image resembles the ethanol case for low collision energy. Fig. 9 shows the translational energy release and angular distributions. Again we see that the energy release is not to the thermodynamic limit.

Table I summarizes the results for all the alcohols studied in this experiment. All the translational energy distributions peak around 6 kcal/mol, irrespective of the alcohol reagent and

collision energy. Another common thread is that the fraction of energy going into translation is similar for all the alcohols.

## DISCUSSION

The reaction of methanol with chlorine atoms has been studied in a number of laboratories using traditional kinetic methods<sup>51</sup> and the consensus is that the hydroxymethyl radical formation channel is predominant. The rate of reaction is moderately fast,  $(5.3-6.3) \times 10^{-11} \text{ cm}^3 \text{ molecule}^{-1} \text{ s}^{-1}$ , with no appreciable barrier. There has been no experimental study on the dynamics of H abstraction from methanol. However Jodkowski *et al*<sup>51</sup> have performed ab-initio calculations at different levels of theory and using several basis sets to characterize stationary points on the potential surface for the reaction of Cl with CH<sub>3</sub>OH. They found several minima, including one in the entrance channel corresponding to Cl attaching to the O atom and another in the exit channel resembling a hydrogen bonded complex between HCl and CH<sub>2</sub>OH, with the latter representing the minimum point on the surface, 10.0 kcal/mol below the reactants. The presence of these minima led them to suggest that reaction occurs via formation of an intermediate complex similar to the CH<sub>3</sub>OH + F reaction<sup>52</sup>. No exit-barrier was found in their calculation for the CH<sub>2</sub>OH + HCl channel. However, they generated only a few stationary points on the surface and did not explicitly consider the reaction path. Our results clearly show the importance of a direct reaction mechanism, at least at our 8.7 kcal/mol collision energy since we see enhanced sideways-backscattered scattering distributions. We interpret the angular distributions as implying direct close (low, but finite impact parameter) collisions.

T. Khatoon *et al.*<sup>49</sup> studied the kinetics and mechanism of reaction of Cl with ethanol ( $7.2 \times 10^{13} \text{ cm}^3/\text{mol s}$ ) and 1- and 2- propanol. For the reaction of Cl atoms with alcohols, the authors saw no abstraction from the OH group, abstraction from the alkyl groups followed the thermodynamically favored route by forming mainly secondary radicals. J. Edelbuttel-Einhaus *et*

al report a rate constant of  $4.72 \times 10^{13} \text{ cm}^3/\text{mol s}$  and obtain a branching ratio of 1:20 between reaction 4 and 3 confirming that the 1-hydroxyethyl radical is predominantly formed.

The scattering studies on ethanol allow us to compare the effect of collision energy. At low collision energy, scattering is predominantly in the backward hemisphere. With an increase in collision energy the scattering is enhanced in the sideways direction with no concomitant increase in the translational energy release. The angular distributions for ethanol at the higher collision energy begins to resemble that of methanol, suggesting that finite impact parameter collisions begin to play a role, or deviations from collinearity may be more important. The translational energy release is reduced in the sideways direction, implying greater internal energy in the larger impact parameter collisions. This is consistent with greater rotational excitation for these side-ways scattered products.

The energies of the C-H bonds in ethanol and propane are very similar, furthermore the structures resemble each other. This allows us to compare the results for Cl-C<sub>2</sub>H<sub>5</sub>OH with Cl-C<sub>3</sub>H<sub>8</sub>. We do not observe the large impact parameter dominated forward scattering reported in the case of propane. However, for the low impact parameter sideways-backward scattering there is qualitative agreement with our results. Blank et al<sup>20</sup> saw strong coupling between their angular and translational energy distributions, again this is in agreement with our observations. These authors found a much larger fraction of available energy in translation than in the Cl-ethanol reaction, and this fraction changed little with collision energy ( $\langle E_T \rangle / E_{\text{avail}} = 0.53, 0.52, 0.48$  for  $E_{\text{coll}} = 8.0, 11.5, 31.6 \text{ kcal/mol}$ ). An examination of column 5 in table 1 shows qualitatively similar behavior.

Following in a similar vein, scattering for the Cl-C<sub>3</sub>H<sub>7</sub>OH system should resemble the Cl-C<sub>5</sub>H<sub>12</sub> system. As mentioned in the introduction, Hemmi and Suits<sup>21</sup> invoked the participation of the carbon skeleton in the scattering process to account for the substantial internal energy deposited in the hydrocarbon radical fragment. In the case of the Cl-isopropanol system our

angular distributions are qualitatively quite similar to the backward scattering (channel 2) reported in the Cl-C<sub>5</sub>H<sub>12</sub> system. The authors saw a broad backward scattering distribution with about 35% of the available energy being deposited into product translation; in the Cl-C<sub>3</sub>H<sub>7</sub>OH system we observe 31%. And just as in the propane case, these authors observed a distinct forward-scattered component with almost all the available energy being deposited into product translation.

It is surprising, given the similarity in the sideways-backward scattering between the Cl-alcohol and Cl-hydrocarbon systems, that we do not observe the forward scattering component seen by Suits and co-workers in their Cl-hydrocarbon experiments. As mentioned before we cannot extract quantitative information about forward scattering events since the extensive photodissociation of the parent alcohol blinds us in this sector. However any forward scattering will be superimposed on the photodissociation signal and this should be readily observable in our experiment. A possible reconciliation for the difference between our experiment and those performed on the Cl-hydrocarbon systems may lie in the source of Cl atoms used in the two sets of experiments. We used a photolytic source and have carefully characterised the Cl beam to be of predominantly ground state character. In the Cl-hydrocarbon experiments<sup>21,20</sup> the Cl atom beam was generated by thermal dissociation of Cl<sub>2</sub> in a heated nozzle maintained at 1500-1550°C. A Boltzmann distribution as stated by the authors predicts that ca. 15% of the chlorine atoms will be formed in spin-orbit excited state, Cl (<sup>2</sup>P<sub>1/2</sub>). While the excited state component of the Cl beam was not explicitly determined, the authors assumed that the supersonic expansion would relax the spin-orbit excited component of the beam. Recently Liu and co-workers have seen enhanced reactivity with spin-orbit excited Cl<sup>53</sup> and F<sup>54</sup> atoms. They find the spin-orbit excited atoms show very different dynamical behavior compared to their ground state counterparts. We tentatively suggest that the forward scattering seen in the crossed-beam Cl-hydrocarbon systems may arise from the participation of the spin-orbit excited component of their

Cl. Efforts are underway in this laboratory to study the effect of spin-orbit excitation on the reaction dynamics of alcohols and hydrocarbons.

There is also the possibility, since we use single photon ionization, that internal excitation of the product detected might bias our sensitivity. It is known that internal excitation of species lowers the ionization potential – in our case this would translate to detecting highly vibrationally excited products more efficiently. However an experimental complication in our studies - the alcohol photochemistry - reveals that we are not subject to such bias. We measured the translational energy release of  $\text{CH}_2\text{OH}$  and  $\text{CH}_3\text{CHOH}$  formed in the 157nm photodissociation of  $\text{CH}_3\text{OH}$  and  $\text{CH}_3\text{CH}_2\text{OH}$  respectively. In both cases we found the energy release was to the thermodynamic limit. If we were biased in our detection sensitivity we would not be able to detect the internally cold products. We are thus reassured that we are not subject to internal energy bias in our VUV photoionization crossed-beam velocity map imaging experiment. We intend future measurements to verify this assumption.

These results demonstrate the power of VELMI combined with single-photon VUV ionization. Work is currently underway in our laboratory on reactions with other alcohols, and analogous reactions of O and OH should be quite feasible. With judicious choice of chemical system and probe light sources, the detailed and systematic investigations of the dynamics of many polyatomic reactions should be routine.

### **Acknowledgements**

This paper is fondly dedicated to the memory of the late Professor Roger W. Grice, a continuing inspiration to the practitioners of the crossed-molecular beams technique. We thank Mr. K. Rodriguez (U\*STAR -undergraduate student training in academic research) and Mr. J. McFarlane for technical assistance, and Prof. C. B. Moore for loan of the video integration system. This work was supported by the Director, Office of Energy Research, Office of Basic Energy Sciences, Chemical Sciences Division of the U.S. Department of Energy under contract No. DE-ACO3-76SF00098.

## References:

- (1) Andresen, P., Luntz, A. C. *J. Chem. Phys.* 1980, **72**, 5842.
- (2) Luntz, A. C., Andresen, P. *J. Chem. Phys.* 1980, **72**, 5851.
- (3) Kleinermanns, K., Luntz, A. C. *J. Chem. Phys.* 1982, **77**, 3533.
- (4) Kleinermanns, K., Luntz, A. C. *J. Chem. Phys.* 1982, **77**, 3537.
- (5) Kleinermanns, K., Luntz, A. C. *J. Chem. Phys.* 1982, **77**, 3774.
- (6) Dutton, N. J., Farthing, J. W., Fletcher, I. W., Whitehead, J. C. *Molecular Physics* 1983, **50**, 347.
- (7) Dutton, N. J., Fletcher, I. W., Whitehead, J. C. *Molecular Physics* 1984, **52**, 475.
- (8) Sweeney, G. M., Watson, A., McKendrick, K. G. *J. Chem. Phys.* 1997, **106**, 9172.
- (9) Sweeney, G. M., McKendrick, K. G. *J. Chem. Phys.* 1997, **106**, 9182.
- (10) Simpson, W. R., Orrewing, A. J., Zare, R. N. *Chem. Phys. Lett.* 1993, **212**, 163.
- (11) Simpson, W. R., Rakitzis, T. P., Kandel, S. A., Orrewing, A. J., Zare, R. N. *J. Chem. Phys.* 1995, **103**, 7313.
- (12) Simpson, W. R., Rakitzis, T. P., Kandel, S. A., Levon, T., Zare, R. N. *J. Phys. Chem.* 1996, **100**, 7938.
- (13) Park, J. H., Lee, Y. S., Hershberger, J. F., Hossenlopp, J. M., Flynn, G. W. *J. Am. Chem. Soc.* 1992, **114**, 58.
- (14) Rakitzis, T. P., Kandel, S. A., Levon, T., Zare, R. N. *J. Chem. Phys.* 1997, **107**, 9392.
- (15) Kandel, S. A., Rakitzis, T. P., Levon, T., Zare, R. N. *J. Phys. Chem. A* 1998, **102**, 2270.
- (16) Kandel, S. A., Rakitzis, T. P., Levon, T., Zare, R. N. *J. Chem. Phys.* 1996, **105**, 7550.
- (17) Varley, D. F., Dagdigian, P. J. *J. Phys. Chem.* 1995, **99**, 9843.

- (18) Varley, D. F., Dagdigian, P. J. *Chem. Phys. Lett.* 1996, **255**, 393.
- (19) Varley, D. F., Dagdigian, P. J. *J. Phys. Chem.* 1996, **100**, 4365.
- (20) Blank, D. A., Hemmi, N., Suits, A. G., Lee, Y. T. *Chem. Phys.* 1998, **231**, 261.
- (21) Hemmi, N., Suits, A. G. *J. Chem. Phys.* 1998, **109**, 5338.
- (22) Grosjean, D. *J. Braz. Chem. Soc.* 1997, **8**, 433.
- (23) Lowry, S. O., Devoto, R. S. *Combust. Sci. Tech.* 1976, **12**, 177.
- (24) Reed, T. B., Lerner, R. M. *Science* 1973, **182**, 1299.
- (25) Goldstein, N., Wiesenfeld, J. R. *J. Chem. Phys.* 1983, **78**, 6725.
- (26) Umemoto, H., Kongo, K., Inaba, S., Sonoda, Y., Takayanagi, T., Kurosaki, Y. *J. Phys. Chem. A* 1999, **103**, 7026.
- (27) Bradforth, S. E., Arnold, D. W., Metz, R. B., Weaver, A., Neumark, D. M. *J. Phys. Chem.* 1991, **95**, 8066.
- (28) Ahmed, M., Peterka, D. S., Suits, A. G. *Chem. Phys. Lett* 1999 (submitted).
- (29) Whitaker, B. J. . In *Research in Chemical Kinetics Vol. I*; Compton, R. C. and Hancock, G., Eds.; Elsevier: Amsterdam, 1993.
- (30) Eppink, A., Parker, D. H. *Rev. Sci. Instrum.* 1997, **68**, 3477.
- (31) Ahmed, M., Peterka, D. S., Suits, A. G. *Chem. Phys. Lett.* 1999, **301**, 372.
- (32) Suits, A. G., Bontuyan, L. S., Houston, P. L., Whitaker, B. J. *J. Chem. Phys.* 1992, **96**, 8618.
- (33) Kitsopoulos, T. N., Buntine, M. A., Baldwin, D. P., Zare, R. N., Chandler, D. W. *Science* 1993, **260**, 1605.
- (34) Willis, P. A., Stauffer, H. U., Hinrichs, R. Z., Davis, H. F. *J. Chem. Phys.* 1998, **108**, 2665.
- (35) Willis, P. A., Stauffer, H. U., Hinrichs, R. Z., Davis, H. F. *J. Phys. Chem. A* 1999, **103**, 3706.

- (36) Willis, P. A., Stauffer, H. U., Hinrichs, R. Z., Davis, H. F. *Rev. Sci. Instrum.* 1999, **70**, 2606.
- (37) Stauffer, H. U., Hinrichs, R. Z., Willis, P. A., Davis, H. F. *J. Chem. Phys.* 1999, **111**, 4101.
- (38) Ahmed, M., Blunt, D., Chen, D., Suits, A. G. *J. Chem. Phys.* 1997, **106**, 7617.
- (39) Proch, D., Trickl, T. *Rev. Sci. Instrumen.* 1989, **60**, 713.
- (40) Hemmi, N., Suits, A. G. *J. Phys. Chem. A* 1997, **101**, 6633.
- (41) Arepalli, S., Presser, N., Robie, D., Gordon, R. J. *Chem. Phys. Lett.* 1985, **118**, 88.
- (42) Dobe, S., Berces, T., Temps, F., Wagner, H. G., Ziemer, H. . In *Proceedings of the 25th Symposium (International) on Combustion*; Combustion Institute: Pittsburgh, 1994; pp 775.
- (43) Ruscic, B., Berkowitz, J. *J. Phys. Chem.* 1993, **97**, 11451.
- (44) Ruscic, B., Berkowitz, J. *J. Chem. Phys.* 1991, **95**, 4033.
- (45) Lias, S. G., Bartmess, J. E., Liebman, J. F., Holmes, J. L., Levin, R. D., Mallard, W. G. . In *NIST Chemistry WebBook, NIST Standard Reference Database Number 69* (<http://webbook.nist.gov>); Mallard, W. G., Linstrom, P. J., Eds.; National Institute of Standards and Technology: Gaithersburg MD, 1998.
- (46) Ruscic, B., Berkowitz, J. *J. Chem. Phys.* 1994, **101**, 10936.
- (47) Dyke, J. M., Groves, A. P., Lee, E. P. F., Niavarani, M. H. Z. *J. Phys. Chem. A* 1997, **101**, 373.
- (48) Curtiss, L. A., Lucas, D. J., Pople, J. A. *J. Chem. Phys.* 1995, **102**, 3292.
- (49) Khatoon, T., Edelbutteleinhaus, J., Hoyermann, K., Wagner, H. G. *Ber. Bunsenges. Phys. Chem.* 1989, **93**, 626.
- (50) Williams, J. M., Hamill, W. H. *J. Chem. Phys.* 1968, **49**, 4467.



(51) Jodkowski, J. T., Rayez, M. T., Rayez, J. C., Berces, T., Dobe, S. *J. Phys. Chem. A* 1998, **102**, 9230.

(52) Jodkowski, J. T., Rayez, M. T., Rayez, J. C., Berces, T., Dobe, S. *J. Phys. Chem. A* 1998, **102**, 9219.

(53) Lee, S. H., Lai, L. H., Liu, K. P., Chang, H. *J. Chem. Phys.* 1999, **110**, 8229.

(54) Liu, K. P., Personal Communication.

TABLE 1

| ROH                              | $E_{\text{coll}}^{\text{a}}$<br>(kcal/mol) | $E_{\text{avl}}^{\text{b}}$<br>(kcal/mol) | $\langle E_{\text{tr}} \rangle^{\text{c}}$<br>(kcal/mol) | $f_{\text{tr}}^{\text{d}}$ | $\Gamma_{\text{side/back}}^{\text{e}}$ |
|----------------------------------|--|---|--|----------------------------|--|
| CH <sub>3</sub> OH               | 8.7  | 15.5                                      | 6.1  | 0.39                       | 1.75                                   |
| C <sub>2</sub> H <sub>5</sub> OH | 6.0  | 14.2                                      | 5.4  | 0.38                       | 1.23                                   |
| C <sub>2</sub> H <sub>5</sub> OH | 9.7  | 17.9                                      | 5.7  | 0.32                       | 1.64                                   |
| C <sub>3</sub> H <sub>7</sub> OH | 11.9                                       | 21.9                                      | 6.8  | 0.31                       | 1.33                                   |

<sup>a</sup> Collision energy.

<sup>b</sup> Total energy available.

<sup>c</sup> Average translational energy release.

<sup>d</sup> Fraction of total energy appearing in translation.

<sup>e</sup> Ratio of side-scattered to backscattered flux (see text).

## Figure Captions

1. Schematic of crossed-beam VELMI apparatus.
2. Raw image for 1-hydroxyethyl ( $\text{CH}_3\text{CHOH}$ ) radical product of crossed-beam  $\text{Cl-C}_2\text{H}_5\text{OH}$  reaction at 9.7 kcal/mol collision energy.
3. Data image for hydroxymethyl ( $\text{CH}_2\text{OH}$ ) radical product of crossed-beam  $\text{Cl-CH}_3\text{OH}$  reaction at 8.7 kcal/mol collision energy.
4. Translational energy (top) and angular distribution (bottom) for hydroxymethyl radical from image data in Fig. 3. Forward scattered ( $0^\circ$ ) corresponds to the methanol beam direction.
5. Data images for 1-hydroxyethyl ( $\text{CH}_3\text{CHOH}$ ) radical product of crossed-beam  $\text{Cl-C}_2\text{H}_5\text{OH}$  reaction at 6.0 kcal/mol (A) and 9.7 kcal/mol collision energy (B).
6. Translational energy (top) and angular distribution (bottom) for 1-hydroxyethyl radical from image data in Fig. 5. Forward scattered ( $0^\circ$ ) corresponds to the ethanol beam direction. Solid line  $E_{\text{coll}} = 6.0$  kcal/mol, dashed line  $E_{\text{coll}} = 9.7$  kcal/mol.
7. Translational energy distribution for sideways (dashed line) and back-scattered (solid line) component of 2-hydroxyethyl radical product of crossed-beam  $\text{Cl-C}_2\text{H}_5\text{OH}$  reaction at 6.0 kcal/mol.
8. Data image for hydroxy-isopropyl ( $(\text{CH}_3)_2\text{COH}$ ) radical product of crossed-beam  $\text{Cl-2-C}_3\text{H}_7\text{OH}$  reaction at 11.9 kcal/mol collision energy. Forward scattered ( $0^\circ$ ) corresponds to the propanol beam direction.
9. Translational energy (top) and angular distribution (bottom) for hydroxy-isopropyl radical from image data in Fig. 8. Forward scattered ( $0^\circ$ ) corresponds to the 2-propanol beam direction.

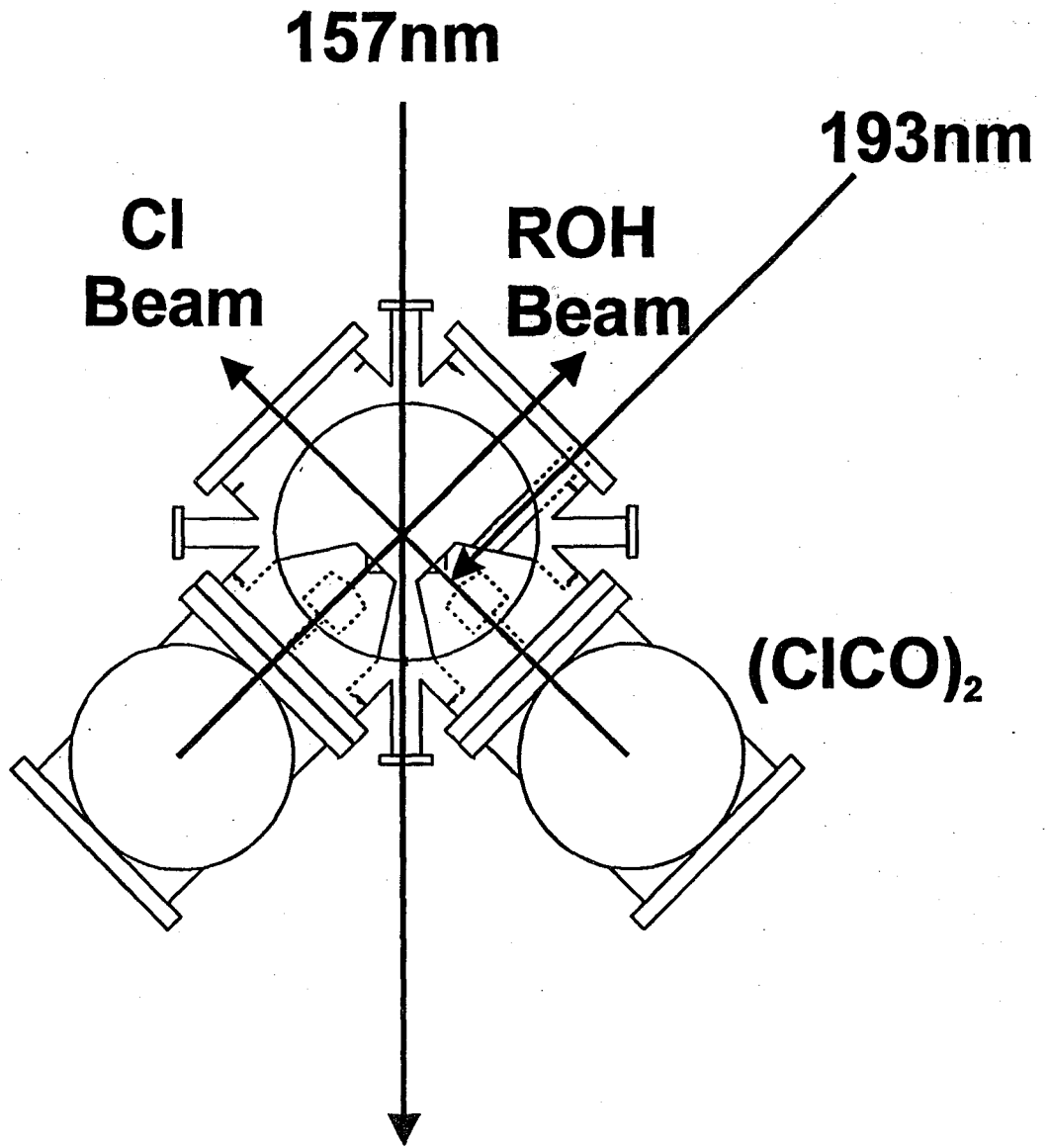


Figure 1

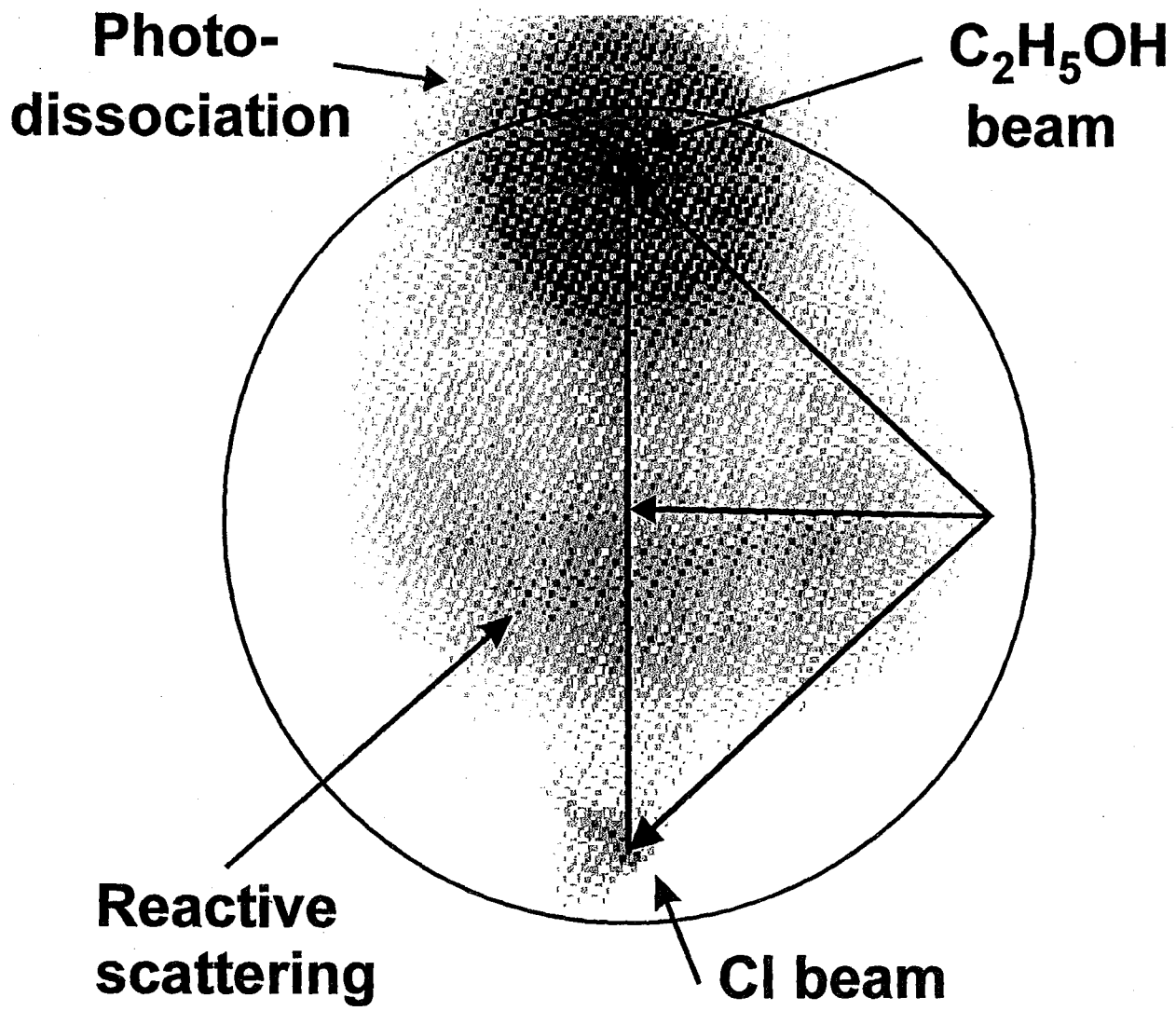


Figure 2

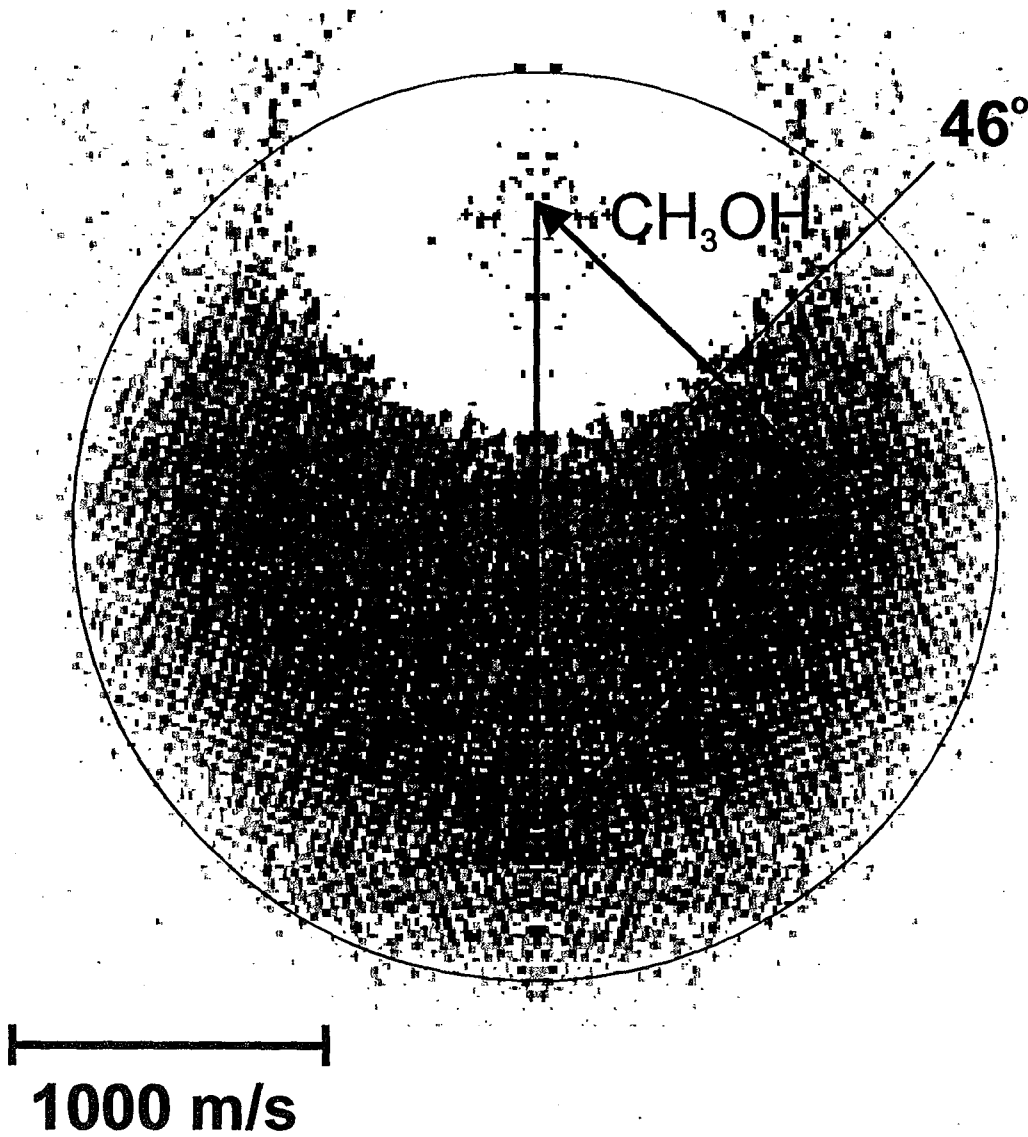
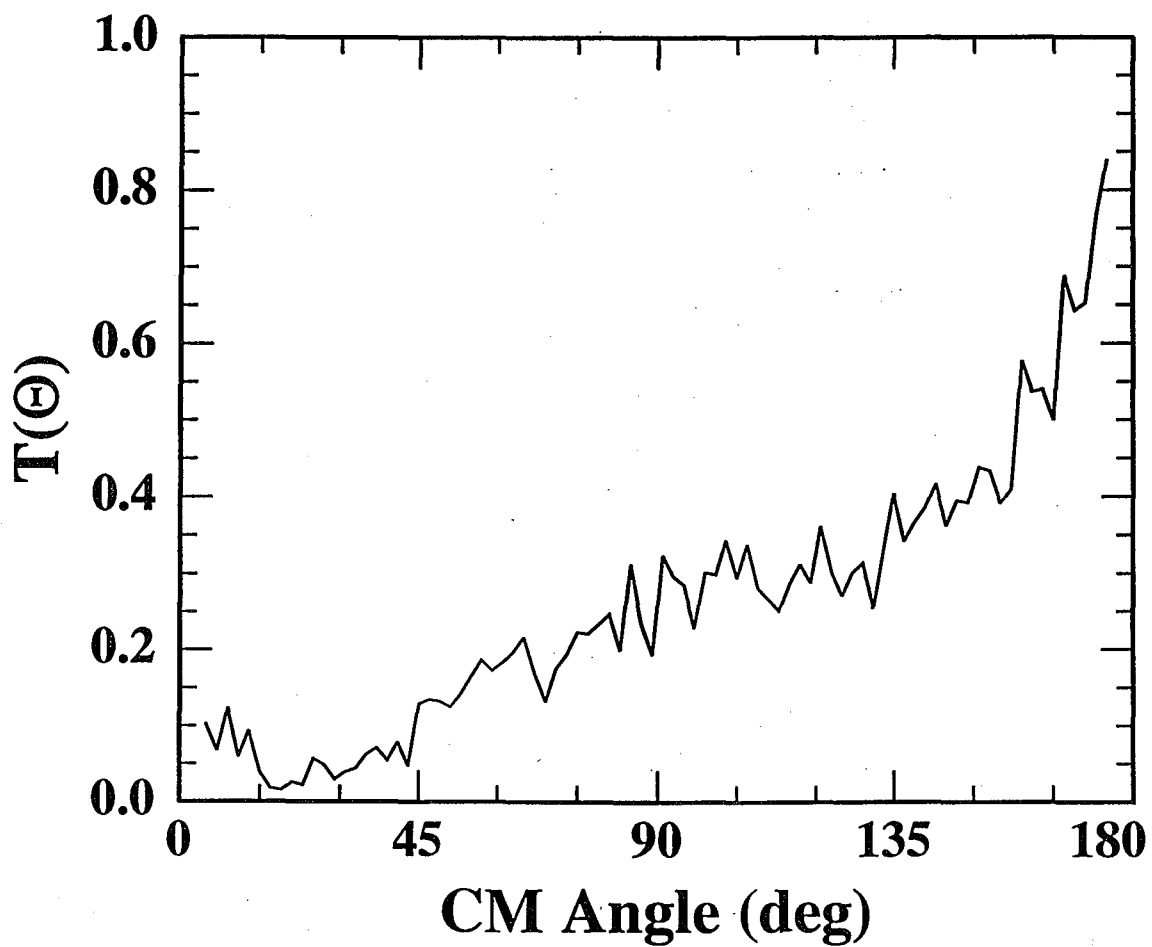
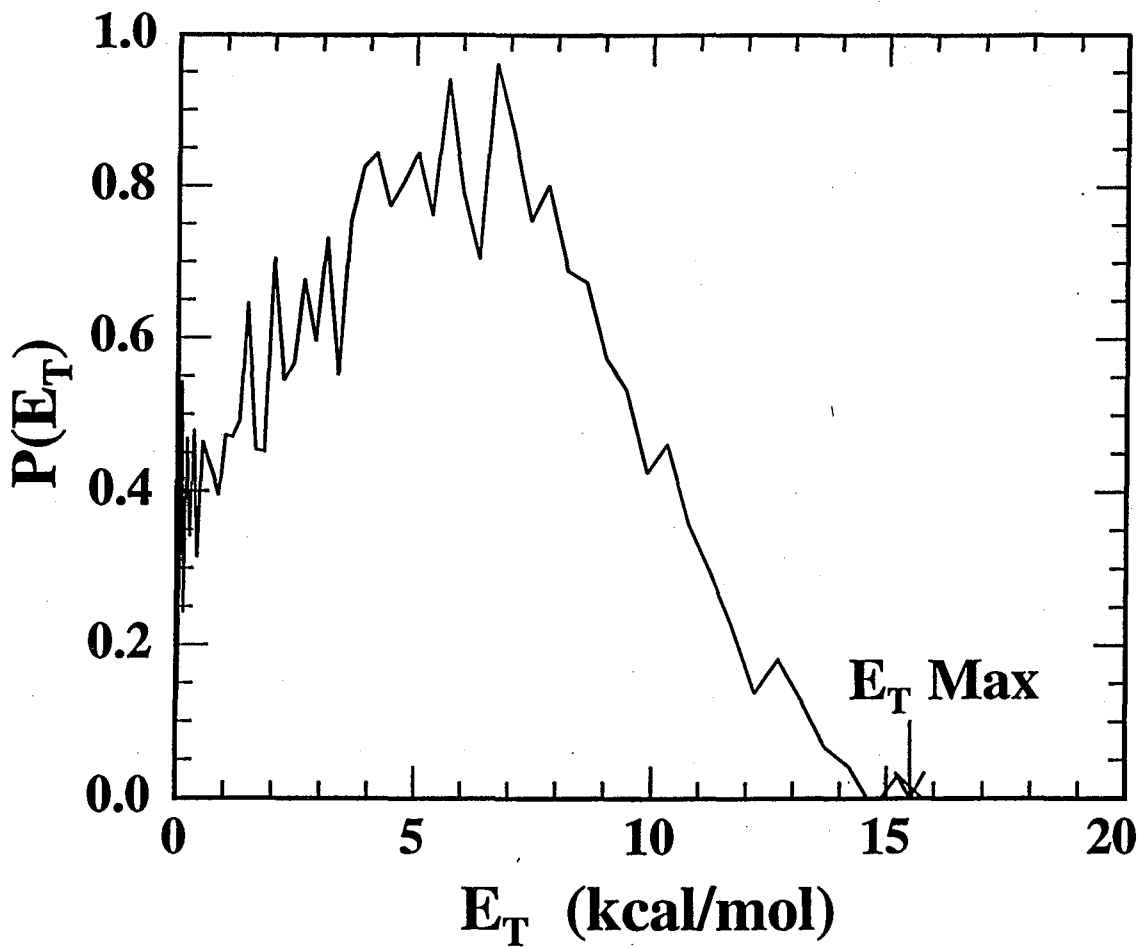
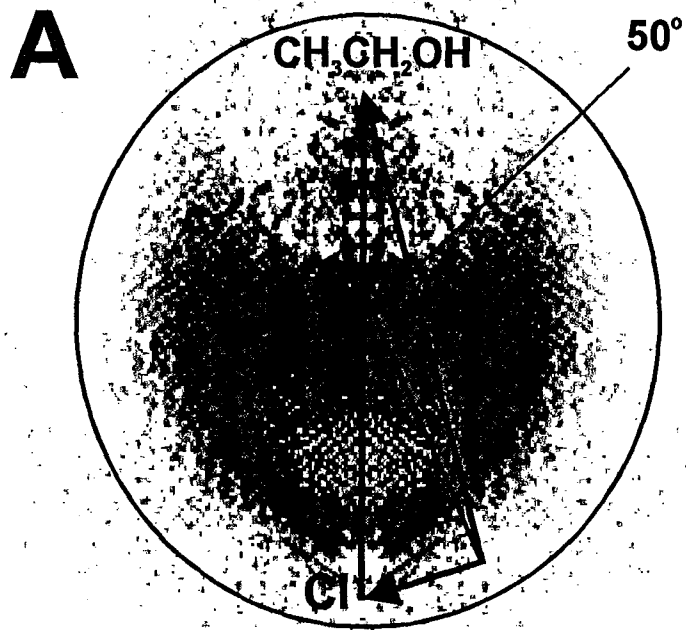


Figure 3





1000 m/s

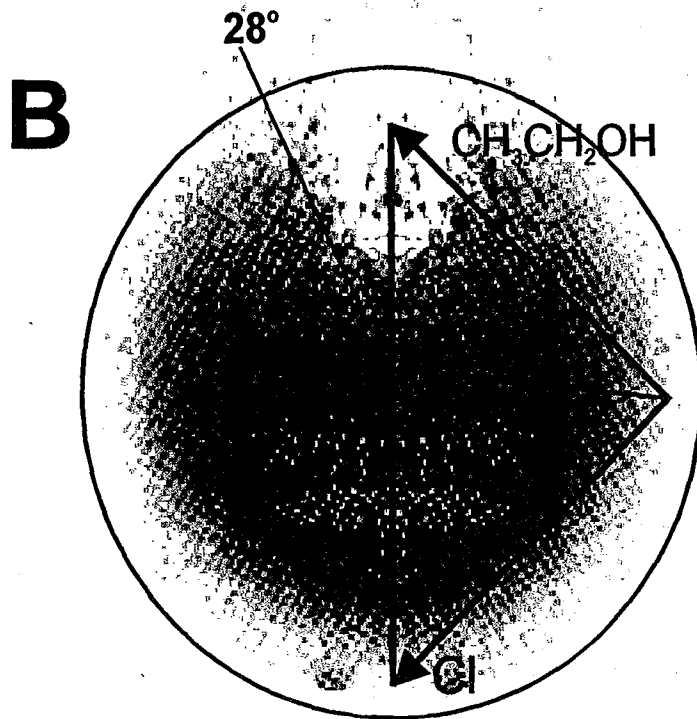
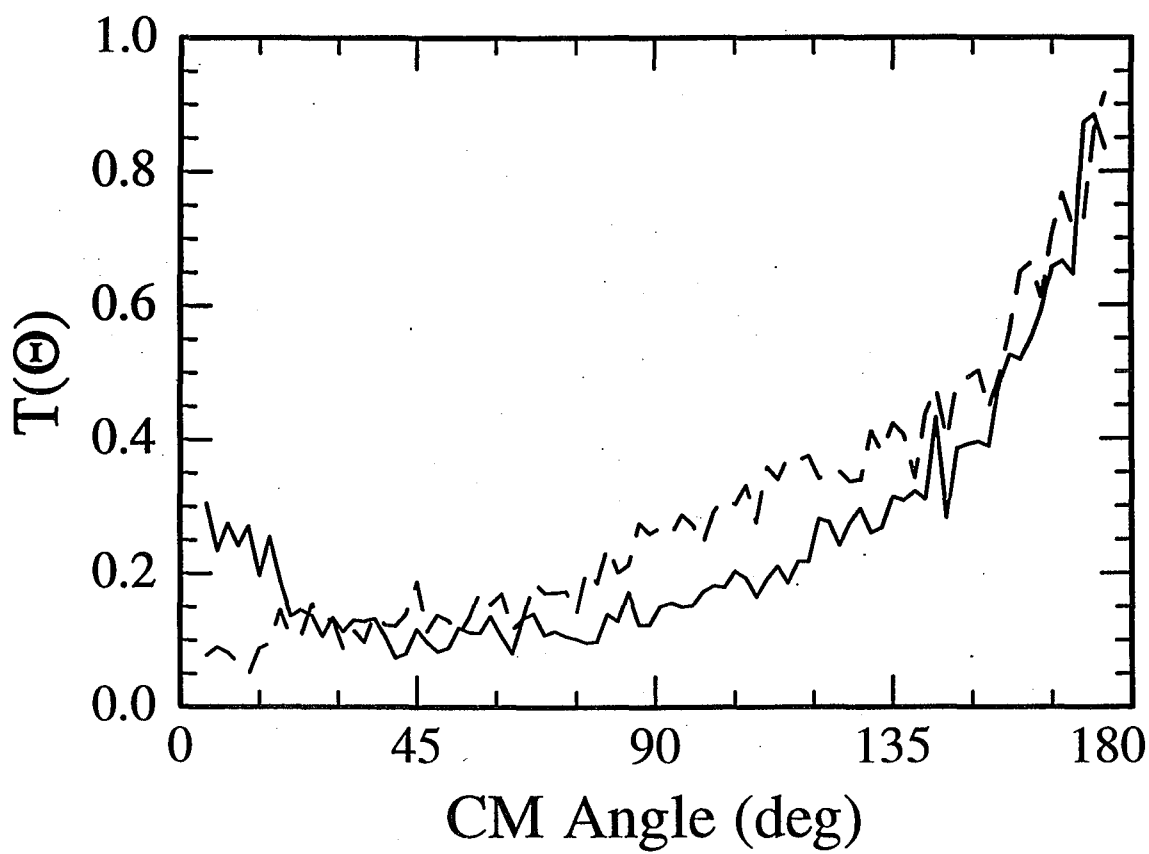
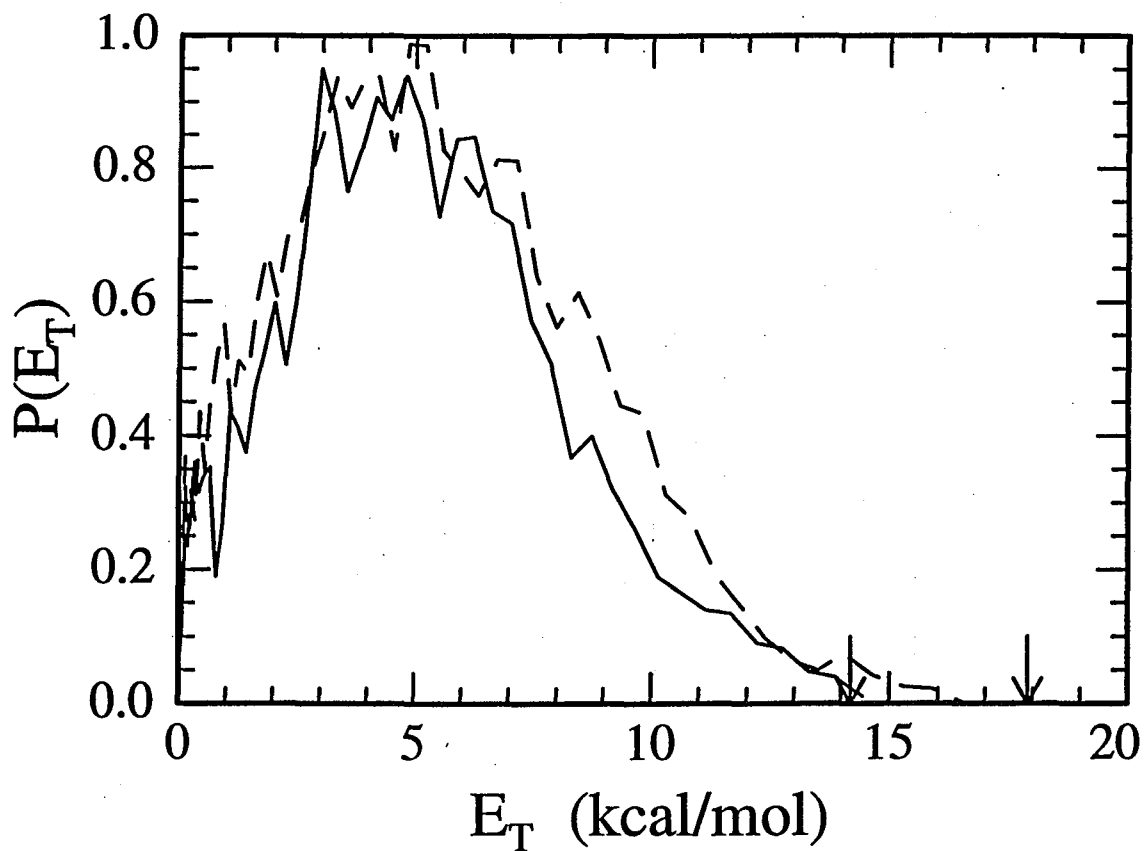


Figure 5





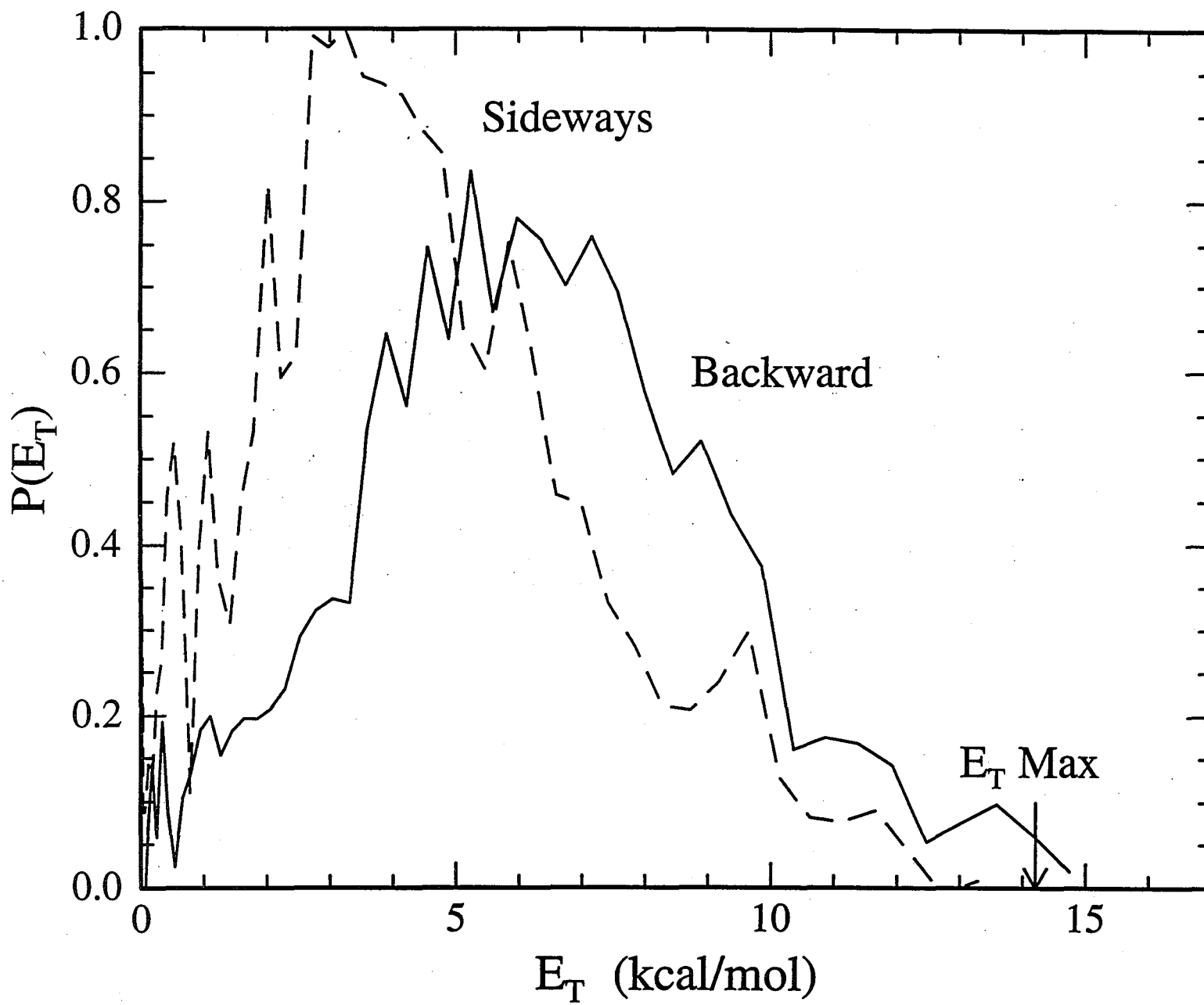


Figure 7

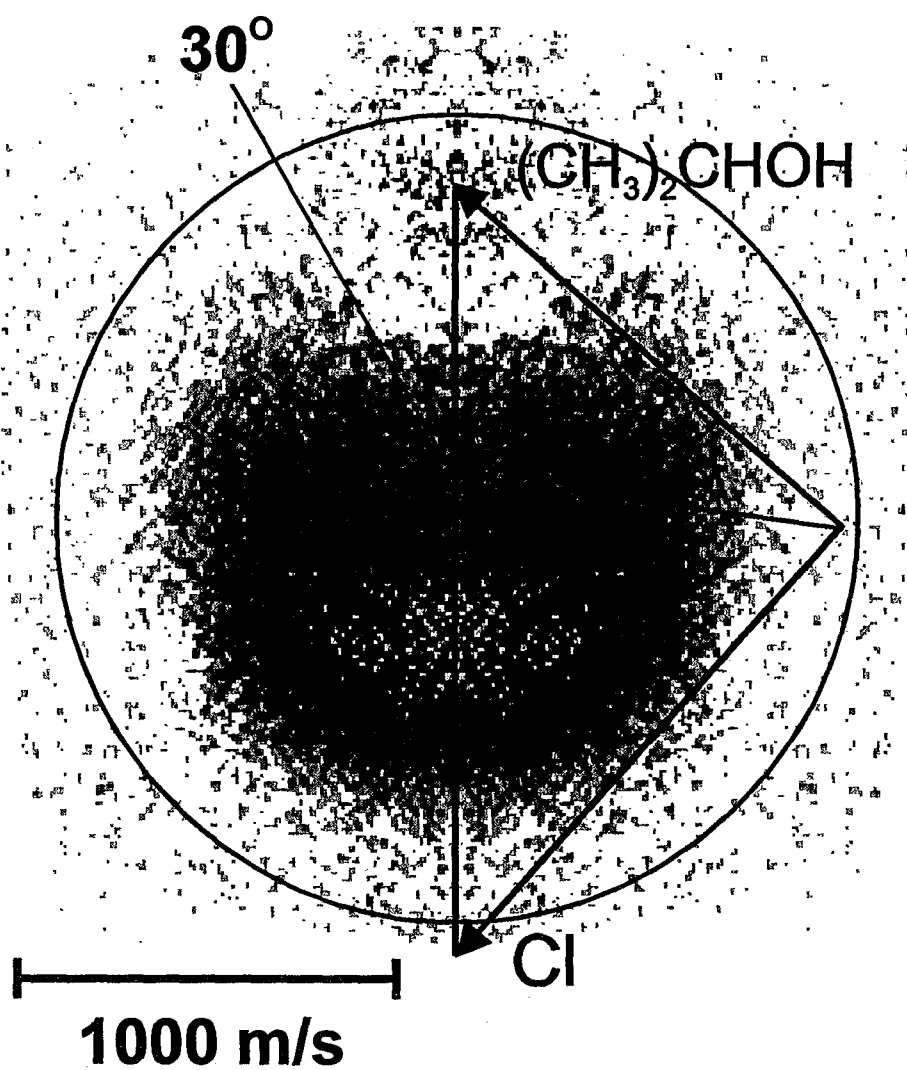


Figure 8

